

Article

Effects of Ventilation Fans and Type of Partitions on the Airflow Speeds of Animal Occupied Zone and Physiological Parameters of Dairy Pre-Weaned Calves Housed Individually in a Barn

Wanying Zhao ^{1,2}, Christopher Y. Choi ³, Xinyi Du ¹, Huiyuan Guan ¹, Hao Li ^{1,*} and Zhengxiang Shi ¹

¹ Department of Agricultural Structure and Bioenvironmental Engineering, College of Water Resources & Civil Engineering, China Agricultural University, Beijing 100083, China; zhaowanying0418@foxmail.com (W.Z.); duxinyi2018@163.com (X.D.); 131259130@163.com (H.G.); shizhx@cau.edu.cn (Z.S.)

² China Rural Technology Development Center, Beijing 100045, China

³ Department of Biological Systems Engineering, University of Wisconsin-Madison, 460 Henry Mall, Madison, WI 53706, USA; cchoi22@wisc.edu

* Correspondence: leehcn@hotmail.com

Abstract: Calves raised in barns are usually kept in individual pens separated by either solid or mesh partitions. To quantify the effects that the two types of partition have on airflow speed in an axial-ventilated-barn, the indoor environment of a calf barn was simulated using computational fluid dynamics (CFD) with validation accomplished by means of direct measurement. To ascertain the effects that two types of partition have on the physiological parameters and health of pre-weaned calves, 24 calves (3–11-day-olds) were selected, equally divided into four groups and sequestered as follows: calves placed in pens separated by solid partitions receiving “low-speed” or “high-speed” airflow; calves separated by mesh partitions receiving “low-speed” or “high-speed” airflow. The results of the CFD simulation showed that the percentage of airflow speed that exceeded 0.5 m s^{-1} at a height of 0.4 m above the floor of the animal occupied zone where calves were separated by mesh partitions was 88%, while the speed was 66–70% for calves separated by solid partitions. The duration of treatment provided to the calves in the MP-LA (mesh partitions and subjected to a low-speed airflow) and MP-HA (mesh partitions and subjected to a high-speed airflow) groups, were both lower than the SP-LA (solid partitions and subjected to a low-speed airflow) and SP-HA (solid partitions and subjected to a high-speed airflow) groups. We conclude that when the fan is operating, contact between calves separated by mesh partitions produces no negative impact on the health of calves; furthermore, this arrangement can provide a higher airflow speed than that delivered to calves raised in pens separated by solid partitions, especially to those calves in pens farther from the fans.

Keywords: ventilation; computational fluid dynamics (CFD); mesh partitions; solid partitions; health status



Citation: Zhao, W.; Choi, C.Y.; Du, X.; Guan, H.; Li, H.; Shi, Z. Effects of Ventilation Fans and Type of Partitions on the Airflow Speeds of Animal Occupied Zone and Physiological Parameters of Dairy Pre-Weaned Calves Housed Individually in a Barn. *Agriculture* **2023**, *13*, 1002. <https://doi.org/10.3390/agriculture13051002>

Academic Editor: Panos Panagakis

Received: 5 April 2023

Revised: 26 April 2023

Accepted: 29 April 2023

Published: 1 May 2023



Copyright: © 2023 by the authors. Licensee MDPI, Basel, Switzerland. This article is an open access article distributed under the terms and conditions of the Creative Commons Attribution (CC BY) license (<https://creativecommons.org/licenses/by/4.0/>).

1. Introduction

A calf raised in an individual pen inside a barn can be managed more precisely and receive better protection from infectious diseases, particularly if the holding pen is enclosed by solid partitions, which prevent nose-to-nose contact [1,2]. Perhaps for this reason, some dairy farmers use individual pens to raise calves separated by solid partitions year around. Lago et al. [3] have suggested that this practice is ideal during months when temperatures fall below a calf’s thermoneutral zone, recommending that, to cope with higher temperatures, a pen should be enclosed on its two sides by solid partitions (to separate each calf from the next), and by mesh partitions front and back. Other than this study, few others have sought to determine the type of partition best suited to housing calves in summer when ambient temperatures are such that temperatures never fall below the upper critical thermoneutral zone of a pre-weaned calf, which will typically range from

26 to 32 °C [4,5], and the physiological range of a calf's body temperature, which will range from 38.1 to 39.3 °C, with diurnal variation [6].

To guard against heat stress, fans can be used to increase the speed of airflow and increase convective heat loss from the skin [7]. As long as the ventilation is sufficient (maintained air velocities above 3 m s⁻¹) and directed to flow over the animals' bodies, this measure can effectively reduce or alleviate heat stress [8]. However, if the fans are arranged to propel air in a direction perpendicular to individual pens separated by solid partitions, the airflow will only benefit those animals in the first few pens [9]; consequently, those calves kept in pens farther from the fans will run a higher risk of developing heat stress. Zhao et al. [10] found that, in a fan-driven ventilation barn, the animal occupied zone (AOZ) of calves separated by mesh partitions received higher airflow speeds than an AOZ divided into pens separated by solid partitions. So far as we know, however, no studies have fully explored or sought to visualize the effects that fan-driven ventilation may have on calves separated by either mesh or solid partitions.

While direct testing can produce meaningful results, field measurements are typically acquired via a method involving point measuring. Computer-generated simulations, on the other hand, which are typically created using computation fluid dynamics (CFD), can provide whole-field data and, thus, provide a far more comprehensive representation of the airflow inside a structure. For this reason, many recent studies have used CFD simulations to predict the efficiency of proposed systems intended to ventilate dairy buildings [11,12]. One such study, Zhou et al. [13], found that an airflow baffle optimally placed inside a low-profile cross-ventilation barn could increase the velocity of air passing through the AOZ. The same study also determined that the rate at which heat was removed from the cows was significant. In an effort to increase the natural ventilation efficiency inside a small-scale calf barn, Norton et al. [14–16] were able to use CFD to predict that the system's performance could be optimized by changing the eave opening using a CFD-generated heat transfer model of a dairy calf.

In a fan-ventilated barn, both the airflow speed and the level of social contact engaged in by the animals depend on the type of partition used to separate the animals. Calves raised in pens separated by mesh partitions on four sides, for example, will typically be afforded more opportunities for social contact than will those raised in holding pens separated by solid partitions on two sides. Mesh partitions also allow for greater airspeed throughout the AOZ. However, more frequent social contact, especially the closely direct physical contact that will occur among pre-weaned calves separated by mesh partitions, can negatively affect the health of the animals, while, on the other hand, the low and even nonexistent airflows that occur when solid partitions separate the calves, may also produce adverse health outcomes. Zhao et al. [10] found that, in summer, still air (an airflow speed < 0.2 m s⁻¹) may impair the immune functions of calves in the 0.5-month-old to 1.5-month-old age range. Further, during the warm seasons, direct contact was significantly more likely to disseminate germs and, thus, spread infections [17,18]. Limiting the level of social contact would, therefore, seem a sensible way to limit the direct transmission of pathogens; however, some studies have found no evidence that unlimited social contact poses a greater threat. Svensson et al. [19], for example, found that pre-weaned calves housed in small groups actually registered a lower incidence of respiratory disease than did calves housed in individual pens, and [20–22] both found that "pair housing" calves produced no negative effect on the occurrence of either diarrhoea or respiratory disease (in comparison with occurrences among individually-housed calves).

Given the limitations of these studies' findings, it would seem that additional research should seek to determine whether pens separated by mesh partitions have a significant negative effect on the health status of calves during warm seasons. Consequently, the objectives of this study were to (1) describe the distribution of airflow speeds occurring throughout the AOZ inside a fan-ventilated calf barn; (2) model an actual barn divided into individual pens, with one version of pens separated by mesh partitions and another version by solid partitions, and compare the airflow speed distribution produced by field

measurements with that predicted by these CFD models; (3) determine the effects on the respiratory rate, rectal temperature and health status of calves housed in these pens, depending on whether a fan-driven airflow passed through an AOZ comprised of either solid-walled pens or mesh-walled pens.

2. Materials and Methods

2.1. Calf Barn

Field experiments were conducted in a commercial barn used to house pre-weaned calves (3234' N, 12054' E) and located in Yancheng, Jiangsu, China; the structural details of the barn and the style of calf management practiced, which are depicted in Figure 1a,b, were identical to those described in Zhao et al. [10].

2.2. CFD Simulation

2.2.1. Geometry

The model barn used in the study was identical to the experimental test barn described in Figure 1a,b. Four models were generated, one for each case study: (1) two solid partitions, one on either side of each pen with no calves present; (2) four mesh partitions enclosing each pen with no calves present; (3) two solid partitions, one on either side of each pen with calves present; (4) four mesh partitions enclosing each pen with calves present. In models 1 and 3, the mesh partitions at the front and back of each holding pen were disregarded, because they were oriented parallel to the airflow direction, and, thus, their effect on the airflow was negligible. The computational-model barn was the same width as the prototype, while the length was appropriately shortened. Each model depicted 3 rows of pens and 3 lines of fans operating simultaneously, as shown in Figure 2a–d; these fans were located in the A zone, as shown in Figure 1b. The calves used in this study were modelled at a computationally affordable level with simplifications. That is, we used a model of a 1-month-old calf having a volume of 0.05 m³ and a surface area of 1.34 m² [16], and we set the modelled calf as a cylinder with a height of 0.8 m and a radius of 0.09 m because a strong correlation has been found to exist between the dynamics associated with this shape and the shape of an animal's torso when the two are modeled in a virtual wind tunnel [23]. For validating the CFD simulations, model 1 and model 2 were selected.

2.2.2. Governing Equations, Computational Scheme, and Convergence Criteria

Computational simulations were conducted to understand the microenvironment of the experimental calf-rearing barn and to investigate whether the type of partition placed between pens would affect the uniformity of airflow through the AOZ. The amount of heat transfer occurring between the atmosphere and the calf was not considered, and only the airflow field in the calf barn was considered in this study. An ANSYS Workbench (Release 20.1, ANSYS, Canonsburg, PA, USA; ANSYS Inc., 2020) was used to perform the CFD simulations. The continuity and Navier–Stokes equations for airflow simulations are expressed in a discretized form throughout the description of the finite volume method. The conservation equations (Equations (1) and (2)) for each of these physical variables are as follows:

Mass conservation equation:

$$\nabla \cdot (\rho \vec{v}) = S_m \quad (1)$$

Momentum conservation equation:

$$\nabla \cdot (\rho \vec{v} \vec{v}) = -\nabla P + \nabla(\vec{\tau}) + \rho \vec{g} + \vec{F} \quad (2)$$

where ρ is the density of air (kg m⁻³), \vec{v} is the velocity (m s⁻¹), s_m is a mass source term that models the vapor release rate by animals (kg m⁻³ s⁻¹), P is the static pressure (kg m⁻¹ s⁻¹),

$\vec{\tau}$ is the stress tensor ($\text{kg m}^{-1} \text{s}^{-2}$), \vec{g} is the gravitational acceleration (m s^{-2}), and \vec{F} is the external force vector (kg m s^{-2}).

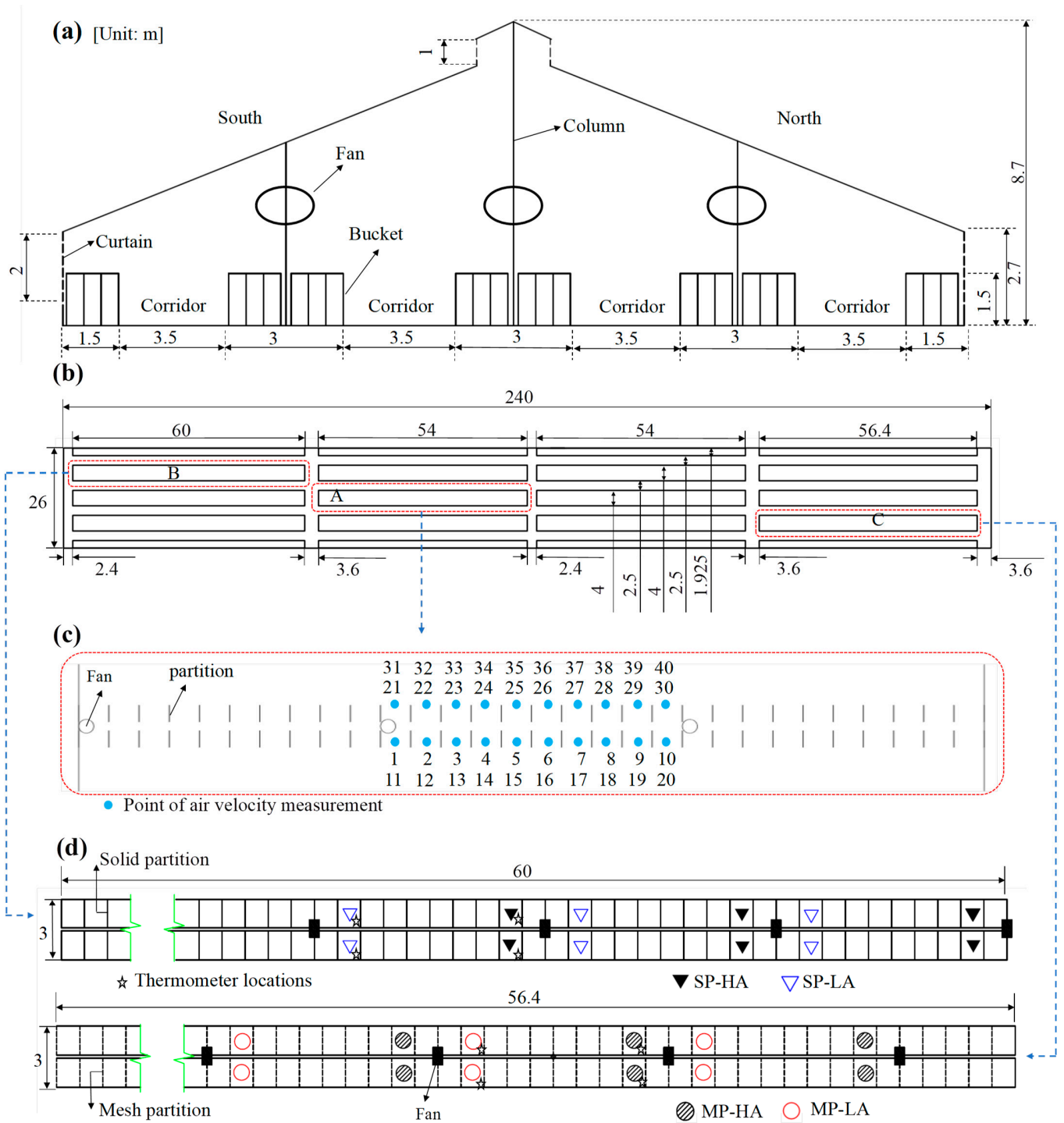


Figure 1. Schematic diagram of experimental calf barn cooled by natural ventilation augmented with axial fans. (a) Side view of experimental barn; (b) floor plan of experimental barn; (c) cross-sectional front view showing locations of the air velocity measurements taken in pens used in the CFD model; (d) detailed plan of pens for housing calf groups (1–4).

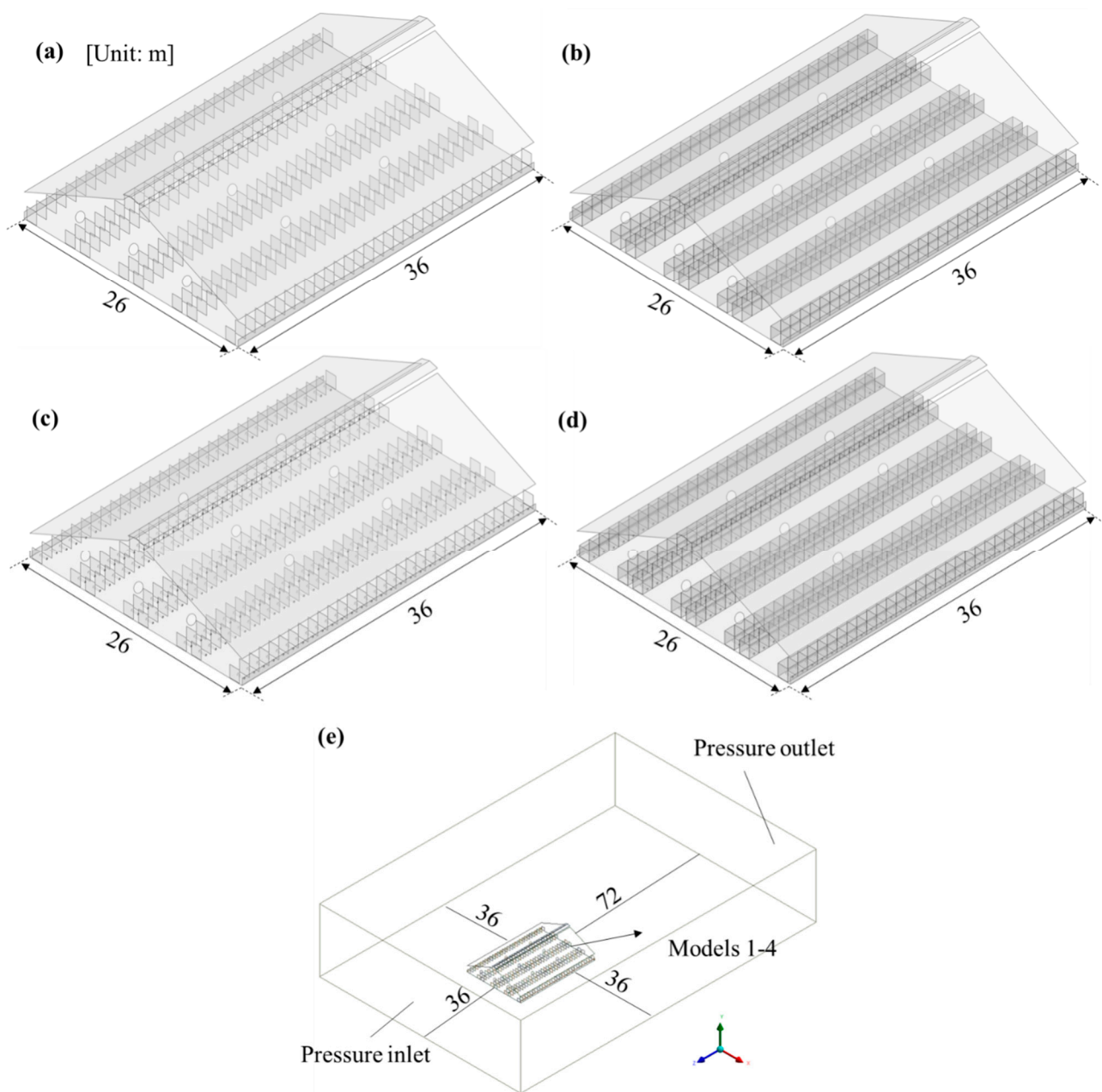


Figure 2. Schematic showing the models: (a–d) perspective view of models 1–4, (e) the surrounding model in the computational domain showing the inlet and outlet locations of the domain.

The k - ϵ models are widely used for simulating the indoor environment because they can be robust and most likely achieve convergence [24]. Meanwhile, in practice, the wall function is widely used due to limitations in computational power [25]. The standard k - ϵ model with standard wall function has been adopted for turbulence modelling, along with turbulent kinetic energy (k) and dissipation rate (ϵ) profiles. The SIMPLE scheme was used to calculate the pressure–velocity coupling, and the second-order upwind discretization schemes were used to calculate the momentum and turbulence energy. After a series of careful tests, the convergence criterion for continuity, x -, y -, z -, k , and ϵ was set to 1×10^{-3} .

2.2.3. Calculating Domain and Boundary Conditions

The computational domain is shown in Figure 2e. Given that the wind was from the z -axis during the experimental measurements, the z -axis-facing side of the computational domain was set as a pressure inlet, while the opposite face of the domain was set as a

pressure outlet (with zero static gauge pressure). The floor, roof, short wall, ridge wall, and modelled calf were all set as no-slip surfaces. The wall boundary condition restricted the flow, and it was assumed that the airflow would enter and leave the domain at a specific pressure (101,325 Pa). Given the fact that the fans had been running for a considerable length of time before the measurements were taken, it was assumed that the airflow had reached a steady state. In addition to the longitudinal air momentum created by the fans, natural ventilation rates (as caused by thermal convection and wind pressure) were also included. When the airspeed inside the barn was tested, the airspeed outside was also tested using a hot-wire anemometer (the values were $<0.02 \text{ m s}^{-1}$), and the temperature and humidity were also tested inside and outside. The results showed that the difference between the inside and outside temperatures was negligible, so the effect produced by temperature difference was assumed to be relatively small. Thus, the effects of wind pressure and heat pressure were not considered.

The fans were modeled using the fan boundary condition based on the fan performance curve. After obtaining the results of a test conducted to ascertain the fan performance curve, the data were fitted to an equation that describes the relationship between the fan pressure rise and the wind speed. In the case of a polynomial, the relationship is best characterized by the following equation:

$$\Delta p_1 = \sum_{n=1}^N f_n v_1^{n-1} \quad (3)$$

where, Δp_1 is the pressure jump (Pa), f_n are the pressure-jump polynomial coefficients, and v_1 is the magnitude of the local air velocity normal to the fan (m s^{-1}). The polynomial of the fan performance curve is described by the following equation:

$$\Delta p_1 = 71.99 + 13.91v_1 \quad (4)$$

To simplify complex blunt body geometries, many CFD experts have developed, tested and used porous media modelling [26]. For example, to investigate airflow and ammonia emissions that occur in livestock buildings, Yin et al. [27] and Rong et al. [28] used a porous media model to represent the slatted floors commonly used in such buildings. Porous media modelling can also drastically reduce the amount of simulation time that would otherwise be required. For example, the barn used in this study contained hundreds of mesh partitions, and each partition was composed of many perforations—so many that to model them would have required a massive amount of computing power. As it was, the solid partitions that separated the pens were replaced by models 1 and 3, which were set as no-slip wall boundaries, and the mesh partitions in models 2 and 4 were set as porous media (Figure 3). The drops in pressure that occur across a mesh partition in the air domain were found for each of six velocities (2, 3, 4, 5, 6, and 7 m s^{-1}), and these were used to obtain the second-order polynomial relationships. Each mesh partition was modelled as a thin porous surface with a finite thickness Δm (0.01 m) over which the pressure change Δp_2 (Pa) was defined as a combination of Darcy's law and an additional inertial loss term as follows:

$$\Delta p_2 = -\left(\frac{\mu}{\alpha} v_2 + C_2 \frac{1}{2} \rho v_2^2\right) \Delta m \quad (5)$$

where, μ is the laminar fluid viscosity (Pa·s), α is the permeability of the partition (m^2), v_2 is the air velocity normal to the porous face (m s^{-1}), ρ is the density of the air (1.25 kg m^{-3}), and C_2 is the pressure-jump coefficient (1 m^{-1}). The flow was solved using the standard k - ϵ turbulence model; Figure 3 shows the mesh partition geometries. The final parameters of the porous media are best described by a fixed-face permeability ($\alpha = 1.72 \times 10^7$) and a pressure-jump coefficient ($C_2 = 159.93$).

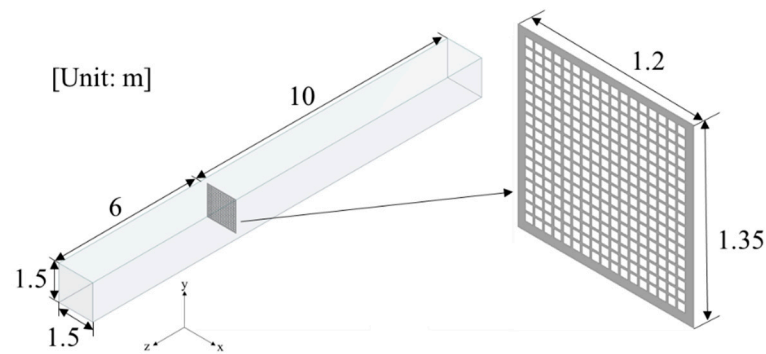


Figure 3. Computational domain for the mesh partition and the geometry.

2.2.4. Computational Grid and Grid Sensitivity analysis

The computational grid was created using an unstructured mesh (Figure 4). To reduce the uncertainty caused by the mesh size, a mesh independence test was performed. For model 1, the mesh within the barn was refined in order to achieve y^+ values of between 30 and 300, and three meshes (11.34, 5.65, and 3.90 million cells) were tested to ensure mesh independency in the results. The average airspeed inside the pen was sampled every meter, and we found that the differences between the 3.90-million-cell mesh and the 5.65-million-cell mesh relative to the 11.34-million-cell mesh were 11.74% and 0.71%, respectively. Therefore, the 5.65-million-cell mesh was considered the best at providing grid-independent results and was used when conducting the remaining simulations.



Figure 4. Mesh of calf barn and air zone in this simulation.

2.3. Validation of CFD Results

The airflow speed measurements needed for CFD validation were collected on 7 June 2020. During the measuring, no calves were present in zone A of Figure 1b. Figure 1c illustrates the locations of the measurement points in zone A. In the case involving pens separated from each other by solid partitions on each side, airflow speed measurements were collected at 40 points located at heights of 0.4 m (points 1–10 and 21–30) and 1.0 m (points 11–20 and 31–40). In the case involving pens separated by mesh partitions, measurements were taken at 20 different points at heights of 0.4 m (points 1–10) and 1.0 m (points 11–20). These two heights were chosen because 1.0 m is the average height of a standing calf's back, and 0.4 m is the average height of a calf's back when lying down. At each point, the airflow speed was measured by averaging readings taken over a 3 min time period, using a multifunctional heat-wire anemometer (9565-P with 964 probe, TSI Inc., Shoreview, MN, USA; $\pm 3\%$ of reading, 0.01 m s^{-1} resolution), at a range of one measurement every second (180 data points), and the time-averaged value was used for comparison with the CFD predictions.

Validation involved making a statistical comparison between the CFD-airflow speed results and the direct measurements. By means of an analysis of variance (ANOVA), the significance of the different variables could be studied.

2.4. Experimental Design

To explore the effects that solid-walled or mesh-walled pens impose on the respiratory rate, rectal temperature and health status of calves subjected to a fan-driven airflow, twenty-four Holstein female calves (3 to 11 days old at the beginning of the test) were selected and divided into four groups, and then each group was treated with a specified ventilation rate (Figure 1d): (1) Group SP-LA calves were separated by solid partitions and subjected to a low-speed airflow (N = 6 calves); (2) Group MP-LA calves were separated by mesh partitions and subjected to a low-speed airflow (N = 6 calves); (3) Group SP-HA calves were separated by solid partitions and subjected to a high-speed airflow (N = 6 calves); (4) Group MP-HA calves were separated by mesh partitions and subjected to a high-speed airflow (N = 6 calves). Each calf was fed 4 L of colostrum within 2 h after birth and 2 L of colostrum in 6–8 h after birth. Each calf was separated from its dam after birth. The total serum protein concentrations of all calves were tested on day 3 and found to be over 5.2 g L^{-1} , which indicated that passive immunization had been successfully acquired from the colostrum.

Eight digital data loggers (HOBO U23 Pro v2; Onset Computer Co., Ltd., Bourne, MA, USA; temperature accuracy of $\pm 0.25 \text{ }^\circ\text{C}$, range: -40 to $70 \text{ }^\circ\text{C}$; relative humidity accuracy of $\pm 2.5\%$ from 10% to 90%) were installed inside the calf pens to measure the inside air temperature and relative humidity. Each logger was located 1.0 m above the floor (Figure 1d). The outside air temperature and humidity data were obtained from the China Meteorological Data Service Center (<http://data.cma.cn/en>, accessed on 1 July 2020). The temperature–humidity index (THI) was calculated using this formula [29]:

$$\text{THI} = (1.8 T_a + 32) - 0.55 (1 - 0.01 RH) \times (1.8 T_a - 26) \quad (6)$$

where, T_a is the ambient temperature ($^\circ\text{C}$) and RH is the relative humidity (%).

Airflow speeds were measured by averaging the readings taken over a 3 min span using the multifunctional heat-wire anemometer, and the airflow speeds across each pen were measured five times in five days. The airflow in the center of the pens was monitored at 0.4 m and 1.0 m above the floor. The respiratory rate and rectal temperature were measured between 13:00 and 15:00 daily. The respiratory rate was measured by counting flank movements in 30 s and multiplying by 2. The rectal temperature was measured by a digital thermometer. The average daily weight gain (ADWG) achieved by each calf was calculated by subtracting the birth weight from the animal's weight at the end of the test and dividing the difference by age (in days). Incidences of bovine respiratory disease (BRD) and diarrhoea that occurred among the calves were diagnosed and identified. The details concerning these incidences of illness were provided in Zhao et al. [10].

2.5. Statistical Analysis

All analyzes were performed using SPSS software version 17.0 (IBM Corp., Armonk, NY, USA). The descriptive statistics were expressed as mean \pm standard error of mean (SEM). Differences between treatments were deemed statistically significant if the associated p -value < 0.05 .

3. Results

3.1. CFD Simulation and Field-Measurement Comparison

Figure 5 compares the CFD predictions and the velocity point measurements associated with models 1 and 2. In general, good agreement between the measurements and simulations was found. The CFD simulation correctly predicted the velocity measurements obtained experimentally. Using CFD, the relative discrepancy (δ) was calculated by applying the following formula: $\delta = |AS_m - AS_p| / AS_m \times 100\%$, where AS_m and AS_p stand for

the measured airflow speed and the predicted airflow speed, respectively. The average discrepancy between the point measurements and CFD predictions was about 19.53% in model 1, with a maximum of about 43.31% at point 31 and a minimum of about 0.22% at point 27. In model 2, the average discrepancy between the point measurements and CFD predictions was about 14.14%, with a maximum of about 40.9% at point 10 and a minimum of about 1.57% at point 3. The CFD results and direct measurements did not differ significantly. The p -value was 0.94 ($p > 0.05$) in model 1 and 0.85 ($p > 0.05$) in model 2. Mainly at higher airflow speeds (greater than 2.5 m s^{-1}), the CFD overestimated the experimental measurements, while at lower speeds, the CFD underestimated the measurements.

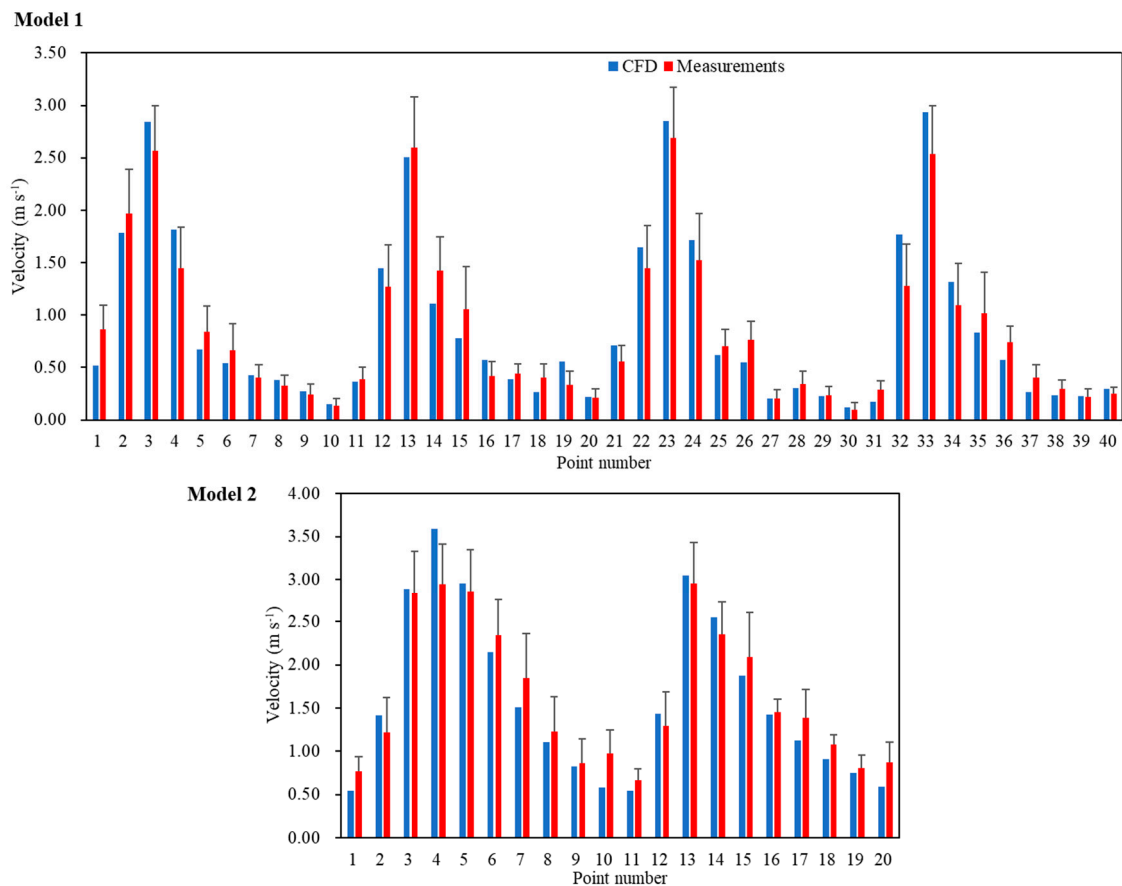


Figure 5. Comparison of the CFD predictions and the field measurements of the air velocity in models 1 and 2. The error bars represent the standard deviation of the measurements.

3.2. Comparison of Airflow Speed Distribution Results in Models 1–4

Figure 6 presents the airspeed distributions on a horizontal plane at heights of 0.4 m and 1.0 m above the floor based on a series of computational simulations, which are depicted in Figure 6a,b, Figure 6c,d, Figure 6e,f, and Figure 6g,h show the airspeed distribution in models 1, 2, 3, and 4, respectively. To better understand the airflow patterns, the wire frames of the model were overlaid on the contours. As expected, in all models, the air speeds recorded in those pens near the fan were higher than those recorded in pens far away from the fan. These findings showed that, in models 1 and 3 with solid partitions, the ventilation fans blowing air perpendicular to the array of pens only provided a sufficient airflow speed ($>1 \text{ m s}^{-1}$) to the first few pens; conversely, in models 2 and 4 with mesh partitions, ventilation fans provided air at a sufficient airflow speed ($>1 \text{ m s}^{-1}$) to most of the holding pens, and the airflow speed supplied to the remaining few pens was mainly between 0.5 m s^{-1} to 1 m s^{-1} . The percentage of airflow speed distribution at the red box line area (Figure 6) at the 0.4 m height and 1.0 m height in models 1–4 are shown in Table 1. At the height of 0.4 m above the floor, the percentage of the area receiving an airflow

speed $\leq 0.5 \text{ m s}^{-1}$ in models 2 (9.04%) and 4 (11.28%) was about one-third that received in models 1 (31.04%) and 3 (30.63%), and the percentage of the area receiving an airflow speed over 1 m s^{-1} in models 2 (80.14%) and 4 (71.13%) was about twice that received in models 1 (47.13%) and 3 (47.77%). At a height of 1.0 m above the floor, more than 94% of the area received an airflow speed greater than 0.5 m s^{-1} in models 2 and 4, while only 65% of the area received an airflow speed greater than 0.5 m s^{-1} in models 1 and 3. The results indicated that, with mesh partitions installed, the fans could provide a high and uniform airflow speed to nearly all of the pens in the AOZ.

Table 1. The airflow speeds and percentage of area covered at heights of 0.4 m and 1.0 m in models 1–4.

Air Velocity (m s^{-1})	0.4 m Height				1.0 m Height			
	Model 1	Model 2	Model 3	Model 4	Model 1	Model 2	Model 3	Model 4
$AS_p \leq 0.5$	31.04%	9.04%	30.63%	11.28%	34.09%	0.85%	34.12%	5.56%
$0.5 < AS_p \leq 1$	21.83%	10.13%	21.60%	17.60%	25.57%	28.94%	23.86%	33.30%
$AS_p > 1$	47.13%	80.84%	47.77%	71.13%	40.34%	70.21%	42.02%	61.14%

Note: AS_p = airflow speed in CFD simulations.

3.3. Environmental Conditions Inside The Barn and the Rectal Temperatures, Respiratory Rates, ADWG, and Health Status of Calves

Throughout the experiment, the average daily temperature and relative humidity ranged from $18.57 \text{ }^\circ\text{C}$ to $28.37 \text{ }^\circ\text{C}$ and 61.93% to 97.92% inside the calf barn, while the average daily temperature and relative humidity outside fluctuated between $17.32 \text{ }^\circ\text{C}$ and $30.46 \text{ }^\circ\text{C}$ and 48.46% and 96.08% , respectively. The average daily THI inside the barn was similar to that recorded outside. In this study, the THI inside the barn ranged between 64 and 78. It should be noted that the welfare of a young calf becomes compromised when the THI rises above 78 when the calf will begin to experience heat stress. Thus, the calves were never in a state of heat stress during this period. The overall variations in temperature, relative humidity, and THI are shown in Figure 7.

According to the data, the airflow speeds did not differ significantly during the five days, which means that each group was essentially subjected to a steady airflow speed. The average data pertaining to airflow speed are shown in Table 2. The calves in group MP-HA received the highest airflow speed, followed by SP-HA, MP-LA, SP-LA ($p < 0.05$). The calves in group SP-LA registered the highest rectal temperatures, and the calves in group SP-HA registered the lowest rectal temperatures. The calves in group SP-LA registered the highest respiratory rate ($p < 0.05$). In addition, the ADWG did not differ significantly among those groups, but the ADWG steadily increased as the airflow speed increased. The total number of sick calves and the duration of treatment in MP-LA and MP-HA was lower than the number of sick calves in SP-LA and SP-HA (Figure 8). The calves in MP-LA suffered the fewest illnesses. The calves separated by mesh partitions received fewer days of treatment than did the calves separated by solid partitions, and the total number of sick and treatment days tallied by the calves of SP-LA was higher than that of the other groups.

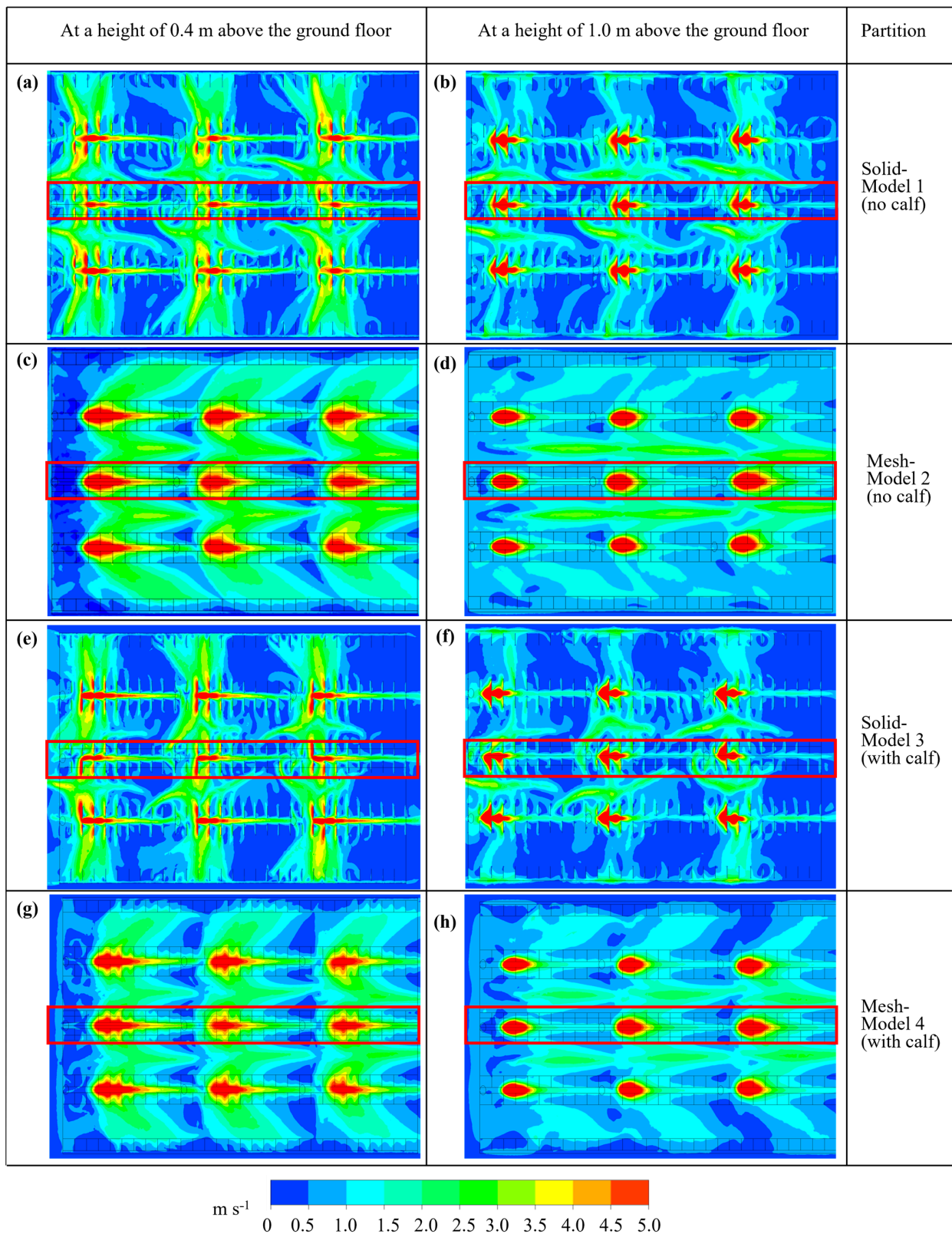


Figure 6. Contours of velocity magnitude in a horizontal plane in the barn: (a,c,e,g) at a height of 0.4 m from the ground floor in models 1, 2, 3, and 4, (b,d,f,h) at a height of 1.0 m from the ground floor in models 1, 2, 3, and 4. The red box zones were calculated based on the percentages of the area with airflow speeds distribution.

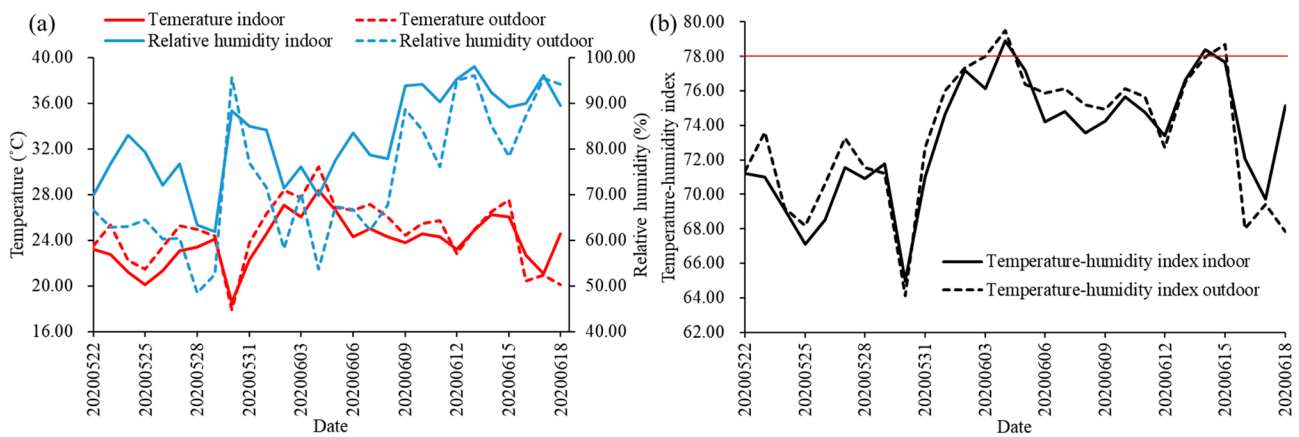


Figure 7. (a) Average daily temperature, relative humidity (RH) and (b) temperature–humidity index (THI) in experimental calf barn and outdoor.

Table 2. Rectal temperatures, respiratory rates, and ADWGs recorded at various airflow speeds (Mean ± SEM).

Group	Airflow Speeds (m s ⁻¹)		Rectal Temperature (°C)	Respiratory Rate (Breaths min ⁻¹)	ADWG (kg d ⁻¹)
	0.4 m	1.0 m			
SP-LA	0.13 ± 0.01 ^d	0.14 ± 0.04 ^d	39.16 ± 0.04 ^a	59.89 ± 1.57 ^a	0.77 ± 0.11
MP-LA	0.65 ± 0.05 ^c	0.61 ± 0.04 ^c	39.13 ± 0.04 ^{ab}	54.06 ± 1.76 ^b	0.83 ± 0.07
SP-HA	2.51 ± 0.50 ^b	2.60 ± 0.11 ^b	38.99 ± 0.04 ^b	51.22 ± 1.62 ^b	0.84 ± 0.67
MP-HA	2.22 ± 0.10 ^a	2.80 ± 0.06 ^a	39.14 ± 0.04 ^{ab}	53.64 ± 1.71 ^b	0.98 ± 0.01

Note: Group SP-LA included those calves separated by solid partitions and receiving a low-speed airflow (far from the fans); Group MP-LA included those calves separated by mesh partitions and receiving a low-speed airflow (far from the fans); Group SP-HA included those calves separated by solid partitions and receiving a high-speed airflow (near the fans); Group MP-HA included those calves separated by mesh partitions and receiving a high-speed airflow (near fans); ADWG = average daily weight gain; ^{a-d} values assigned different letters within the same column represent significant differences (*p* < 0.05).

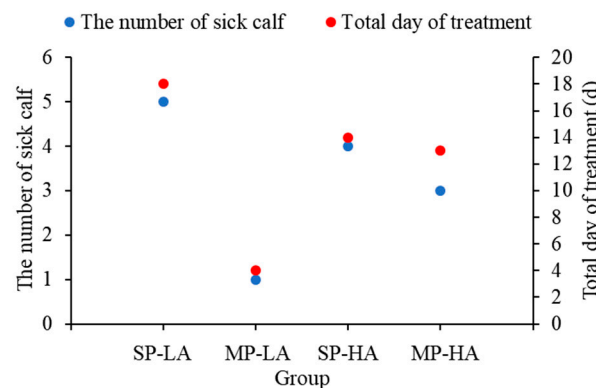


Figure 8. Disease calves and total treatment days during the experiment.

4. Discussion

This study sought to determine the effects that both solid and mesh partitions might have on the speed of an airflow passing through an AOZ inside a calf barn equipped with an axial-fan-ventilated system. Although the two types of partition had been used for many years previous to this study, all that was known was that individually housed calves received different airflow speeds depending on which kind of partition separated them. Moreover, no published scientific literature had reported on efforts to visualize the airflow speed distribution that typically occurred in the AOZ, regardless of whether the pens were separated by solid or mesh partitions. The average discrepancy between the air

speeds predicted by CFD and those measured directly was similar to the 15.5% discrepancy found by a previous study [12] and similar to the difference found by Bustamante et al. [30]. The discrepancy most likely occurred because the direct measuring typically took into account the disruptive actions of workers, which could not be captured by the CFD model. Although discrepancies existed between the model and experimental data, the primary airflow speed was accurately predicted to an acceptable degree, and the discrepancy was deemed insignificant. In other words, either direct measurement or CFD can be used to estimate the airflow speed generated by a fan-driven ventilation system operating inside a calf barn. The interior airflow speed achieved by model 4 (about 88–94% of the AOZ at the heights of 0.4 m and 1.0 m received an air velocity of over 0.5 m s^{-1}) is especially desirable during the recent, increasingly extreme heat waves apparently caused by global warming.

During the experiment, the airflow occurring in the pens of group SP-LA was considered still air—that is, air moving at a speed of less than 0.2 m s^{-1} [31]. According to Zhao et al. [10], such a low air circulation rate can adversely affect the respiratory rate and rectal temperature during warm seasons. Hence (and similar to the findings of that study), the SP-LA calves in this study registered the highest respiratory rates and rectal temperatures. Although a previous study had found that, during the summer season, calves cooled by fans registered lower respiration rates than did calves not cooled by fans [32], the respiratory rates and rectal temperatures recorded in this study did not precisely show a positive correlation between airflow speed and cooling effect, as changes in both were also most likely influenced by each calf's level of health (when a calf becomes ill, its core temperature and breathing rate will commonly rise above the norm).

Calves are especially susceptible to diarrhoea in the first 21 d [33] and to BRD in the first 60 d [34]. Moreover, the prevalence of BRD will begin to increase in week 2 and peak in week 7 [3]. The calves in this study that were separated by mesh partitions required fewer days of treatment than did the calves separated by solid partitions (Figure 8). The bacterial counts registered by the calves kept in pens separated by solid partitions increased as the number of solid partitions around each pen increased ($p < 0.05$), and these counts correlated significantly with the prevalence of respiratory disease [3]. Air drafts, as well as airborne microbiological flora, have also been associated with an increased risk of BRD among herd members [3,35]. Accordingly, the percentage of calves that suffered from BRD when subjected to an air draft $< 0.3 \text{ m/s}$ (14.5%) was greater than when the air draft was $\geq 0.3 \text{ m/s}$ (8.3%) [36]. However, the practice of placing solid partitions between the pens has long been the accepted way to reduce the risk of diseases spread by contact [17]; one study found, for example, that the incidence of respiratory disorders among calves housed in individual pens separated by solid partitions was 38.5%, compared with 60.0% among group-penned calves [37]. It should be noted, however, that this particular study was conducted only in winter. Possibly, the contradictions posed by the other studies can be attributed to the same condition: the work was carried out only during cold weather. Other previous studies have shown that the morbidity rate among calves raised in pairs or in small groups was no higher than that of calves raised in individual pens [21,38,39]. If this is so, then apparently incidental contact should have no negative impact.

5. Conclusions

In this study, we sought to determine the extent to which an airflow passing through the AOZ inside a calf barn might be affected by the kind of partition used to separate the holding pens from each other. The airflow investigated was generated by an axial-fan ventilation system, and two kinds of partition were tested: solid and mesh. The effects of this setup were calculated based on direct measurements and on the predictions achieved by means of numerical simulations created with the help of a computational fluid dynamics technique. Then the two sets of outcomes were compared to determine the degree of agreement. The physiology and health of two groups of dairy calves was also assessed, one group housed in pens separated by mesh partitions and the other in pens separated by solid partitions.

This work resulted in three major findings: (1) in-stall air speeds were obtained, and it appears that a fan-driven airflow passing through the pens separated by mesh partitions could provide airflow speeds above 0.5 m s^{-1} to more than 88% of the pens in the AOZ, while an identical ventilation system could drive the same airflow at the same speeds through an AOZ divided into pens separated by solid partitions, but only about 66% to 70% of the pens would receive air at that rate; (2) whenever the average daily temperature and relative humidity inside the AOZ ranged from $18.57 \text{ }^{\circ}\text{C}$ to $28.37 \text{ }^{\circ}\text{C}$ and 61.93% to 97.92%, respectively, the calves of one particular group (SP-LA, which involved pens separated by solid partitions and arrayed farthest away from the fan) registered an average rectal temperature and respiratory rate that was higher than those of the other groups; (3) the health status of calves was positively affected when they were penned in an AOZ divided by mesh partitions and cooled by a high-speed airflow ($>0.5 \text{ m s}^{-1}$), whereas the health status of calves was negatively affected when they were penned in an AOZ divided by solid partitions and cooled by a low-speed airflow ($<0.2 \text{ m s}^{-1}$).

Given these findings, we were able to conclude that, in warm weather, with the axial-flow fan system operating, calves kept in close proximity in pens separated by mesh partitions will suffer no significant negative health effects as long as the airflow cooling them is maintained at a velocity above 0.5 m s^{-1} . Conversely, a low-speed airflow ($<0.2 \text{ m s}^{-1}$) passing over the same set of pens will increase the risk of disease.

Author Contributions: W.Z.: conceptualization, methodology, software, investigation, writing—original draft, visualization; C.Y.C.: conceptualization, writing—review and editing, supervision; X.D.: investigation; H.G.: investigation. H.L.: writing—review and editing, supervision; Z.S.: supervision. All authors have read and agreed to the published version of the manuscript.

Funding: This research was supported by National Key R & D program Inter-governmental/Hong Kong, Macao and Taiwan key projects (2019YFE0103800) and China Agriculture Research System (CARS-36).

Institutional Review Board Statement: The study was conducted by Institutional Animal Care and Use Committee at China Agricultural University (Beijing, P. R. China; permit no. AW10102020-1-1).

Data Availability Statement: The data presented in this study are available on request from the corresponding author.

Acknowledgments: The authors gratefully acknowledge the help provided by Shenfeng dairy farm in Yancheng, China, where the experiments were carried out.

Conflicts of Interest: The authors declare no conflict of interest.

References

1. Bickert, W.G. *Dairy Freestall Housing and Equipment*, 7th ed.; MidWest Plan Service: Ames, IA, USA, 2000.
2. Gulliksen, S.M.; Lie, K.I.; Loken, T.; Osteras, O. Calf mortality in Norwegian dairy herds. *J. Dairy Sci.* **2009**, *92*, 2782–2795. [[CrossRef](#)] [[PubMed](#)]
3. Lago, A.; McGuirk, S.M.; Bennett, T.B.; Cook, N.B.; Nordlund, K.V. Calf Respiratory Disease and Pen Microenvironments in Naturally Ventilated Calf Barns in Winter. *J. Dairy Sci.* **2006**, *89*, 4014–4025. [[CrossRef](#)] [[PubMed](#)]
4. Neuwirth, J.G.; Norton, J.K.; Rawlings, C.A.; Thompson, F.N.; Ware, G.O. Physiologic responses of dairy calves to environmental heat stress. *Int. J. Biometeorol.* **1979**, *23*, 43–254. [[CrossRef](#)] [[PubMed](#)]
5. Spain, J.N.; Spires, D.E. Effects of supplemental shade on thermoregulatory response of calves to heat challenge in a hutch environment. *J. Dairy Sci.* **1996**, *79*, 639–646. [[CrossRef](#)] [[PubMed](#)]
6. Piccione, G.; Caola, G.; Refinetti, R. Daily and estrous rhythmicity of body temperature in domestic cattle. *BMC Physiol.* **2003**, *3*, 7. [[CrossRef](#)]
7. Spiers, D.E.; Spain, J.N.; Ellersieck, M.R.; Lucy, M.C. Strategic application of convective cooling to maximize the thermal gradient and reduce heat stress response in dairy cows. *J. Dairy Sci.* **2018**, *101*, 8269–8283. [[CrossRef](#)]
8. Shearer, J.K.; Beede, D.K.; Bucklin, R.A.; Bray, D.R. Environmental modifications to reduce heat stress in dairy cattle. III. *Agric. Pract.* **1991**, *12*, 7–18.

9. Nordlund, K.V.; Halbach, C.E. Calf Barn Design to Optimize Health and Ease of Management. *Vet. Clin. N. Am-Food A.* **2019**, *35*, 29–45. [[CrossRef](#)]
10. Zhao, W.Y.; Choi, C.; Li, D.P.; Yan, G.Q.; Li, H.; Shi, Z.X. Effects of Airspeed on the Respiratory Rate, Rectal Temperature, and Immunity Parameters of Dairy Calves Housed Individually in an Axial-Fan-Ventilated Barn. *Animals* **2021**, *11*, 354. [[CrossRef](#)]
11. Tomasello, N.; Valenti, F.; Cascone, G.; Porto, S.M.C. Development of a CFD Model to Simulate Natural Ventilation in a Semi-Open Free-Stall Barn for Dairy Cows. *Buildings* **2019**, *9*, 183. [[CrossRef](#)]
12. Pakari, A.; Ghani, S. Comparison of different mechanical ventilation systems for dairy cow barns: CFD simulations and field measurements. *Comput. Electron. Agric.* **2021**, *186*, 106207. [[CrossRef](#)]
13. Zhou, B.; Wang, X.S.; Mondaca, M.R.; Rong, L.; Choi, C.Y. Assessment of optimal airflow baffle locations and angles in mechanically-ventilated dairy houses using computational fluid dynamics. *Comput. Electron. Agric.* **2019**, *165*, 104930. [[CrossRef](#)]
14. Norton, T.; Grant, J.; Fallon, R.; Sun, D.W. Assessing the ventilation effectiveness of naturally ventilated livestock buildings under wind dominated conditions using computational fluid dynamics. *Biosyst. Eng.* **2009**, *103*, 78–99. [[CrossRef](#)]
15. Norton, T.; Grant, J.; Fallon, R.; Sun, D.W. Assessing the ventilation performance of a naturally ventilated livestock building with different eave opening conditions. *Comput. Electron. Agric.* **2010**, *71*, 7–21. [[CrossRef](#)]
16. Norton, T.; Grant, J.; Fallon, R.; Sun, D.W. Improving the representation of thermal boundary conditions of livestock during CFD modelling of the indoor environment. *Comput. Electron. Agric.* **2010**, *73*, 17–36. [[CrossRef](#)]
17. Callen, R.J.; Garry, F.B. Biosecurity and bovine respiratory disease. *Vet. Clin. Food Anim.* **2002**, *18*, 57–77. [[CrossRef](#)]
18. Razzaque, M.A.; Abbas, S.; Al-Mutawa, T.; Bedair, M. Performance of pre-weaned female calves confined in housing and open environment hutches in Kuwait. *Pak. Vet. J.* **2009**, *29*, 1–4.
19. Svensson, C.; Lundborg, K.; Emanuelson, U.; Olsson, S.O. Morbidity in Swedish dairy calves from birth to 90 days of age and individual calf-level risk factors for infectious diseases. *Prev. Vet. Med.* **2003**, *58*, 179–197. [[CrossRef](#)] [[PubMed](#)]
20. Bučková, K.; Šárová, R.; Moravcsíková, Á.; Špinka, M. The effect of pair housing on dairy calf health, performance, and behavior. *J. Dairy Sci.* **2021**, *104*, 10282–10290. [[CrossRef](#)]
21. Jensen, M.B.; Larsen, L.E. Effects of level of social contact on dairy calf behavior and health. *J. Dairy Sci.* **2014**, *97*, 5035–5044. [[CrossRef](#)]
22. Bolt, S.L.; Boyland, N.K.; Mlynski, D.T.; James, R.; Croft, D.P. Pair housing of dairy calves and age at pairing: Effects on weaning stress, health, production and social networks. *PLoS ONE* **2017**, *12*, e0166926. [[CrossRef](#)]
23. Li, H.; Rong, L.; Zhang, G.Q. Study on convective heat transfer from pig models by CFD in a virtual wind tunnel. *Comput. Electron. Agric.* **2016**, *123*, 203–210. [[CrossRef](#)]
24. Li, H.; Rong, L.; Zhang, G.Q. Reliability of turbulence models and mesh types for CFD simulations of a mechanically ventilated pig house containing animals. *Biosyst. Eng.* **2017**, *161*, 37–52. [[CrossRef](#)]
25. Kondjoyan, A. A review on surface heat and mass transfer coefficients during air chilling and storage of food products. *Int. J. Refrig.* **2006**, *29*, 863–875. [[CrossRef](#)]
26. Doumbia, E.M.; Janke, D.; Yi, Q.Y.; Amon, T.; Kriegel, M.; Hempel, S. CFD modelling of an animal occupied zone using an anisotropic porous medium model with velocity depended resistance parameters. *Comput. Electron. Agric.* **2021**, *181*, 105950. [[CrossRef](#)]
27. Yin, S.; van 't Ooster, B.; Ogink, N.; Groot Koerkamp, P. Assessment of porous media instead of slatted floor for modelling the airflow and ammonia emission in the pit headspace. *Comput. Electron. Agric.* **2016**, *123*, 163–175. [[CrossRef](#)]
28. Rong, L.; Elhadidi, B.; Khalifa, H.; Nielsen, P. Cfd modeling of airflow in a livestock building. In Proceedings of the Clima 2010: 10th Rehva World Congress, Antalya, Turkey, 9–12 May 2010; p. 457.
29. NRC. *A Guide to Environmental Research on Animals*; National Academy of Sciences: Washington, DC, USA, 1971.
30. Bustamante, E.; Calvet, S.; Estellés, F.; Torres, A.G.; Hospitaler, A. Measurement and numerical simulation of single-sided mechanical ventilation in broiler houses. *Biosyst. Eng.* **2017**, *160*, 55–68. [[CrossRef](#)]
31. Wathes, C.M.; Jones, C.D.R.; Webster, A.J.F. Ventilation, air hygiene and animal health. *Vet. Rec.* **1983**, *113*, 554–559.
32. Hill, T.M.; Bateman, H.G., II; Aldrich, J.M.; Schlotterbeck, R.L. Comparisons of housing, bedding, and cooling options for dairy calves. *J. Dairy Sci.* **2011**, *94*, 2138–2146. [[CrossRef](#)]
33. Hoet, A.E.; Nielsen, P.R.; Hasoksuz, M.; Thomas, C.; Wittum, T.E.; Saif, L.J. Detection of Bovine Torovirus and other Enteric Pathogens in Feces from Diarrhea Cases in Cattle. *J. Vet. Diagn. Investig.* **2003**, *15*, 205–212. [[CrossRef](#)]
34. Cantor, M.C.; Neave, H.W.; Costa, J.H.C. Current perspectives on the short- and long-term effects of conventional dairy calf raising systems: A comparison with the natural environment. *Transl. Anim. Sci.* **2019**, *3*, 549–563. [[CrossRef](#)] [[PubMed](#)]
35. Lundborg, G.K.; Svensson, E.C.; Oltenacu, P.A. Herd-level risk factors for infectious diseases in Swedish dairy calves aged 0–90 days. *Prev. Vet. Med.* **2005**, *68*, 123–143. [[CrossRef](#)]
36. Buczinski, S.; Borris, M.E.; Dubuc, J. Herd-level prevalence of the ultrasonographic lung lesions associated with bovine respiratory disease and related environmental risk factors. *J. Dairy Sci.* **2017**, *101*, 2423–2432. [[CrossRef](#)] [[PubMed](#)]
37. Hanekamp, W.J.A.; Smits, A.C.; Wierenga, H.K. Open versus closed barn and individual versus group housing for bull calves destined for beef production. *Livest. Prod. Sci.* **1994**, *37*, 261–270. [[CrossRef](#)]

38. Kung, L.J.; Demarco, S.; Siebenson, L.N.; Joyner, E.; Haenlein, G.F.W.; Morris, R.M. An evaluation of two management systems for rearing calves fed milk replacer. *J. Dairy Sci.* **1997**, *80*, 2529–2533. [[CrossRef](#)]
39. Wormsbecher, L.; Bergeron, R.; Haley, D.; de Passille, A.M.; Rushen, J.; Vasseur, E. A method of outdoor housing dairy calves in pairs using individual calf hutches. *J. Dairy Sci.* **2017**, *100*, 7493–7506. [[CrossRef](#)]

Disclaimer/Publisher’s Note: The statements, opinions and data contained in all publications are solely those of the individual author(s) and contributor(s) and not of MDPI and/or the editor(s). MDPI and/or the editor(s) disclaim responsibility for any injury to people or property resulting from any ideas, methods, instructions or products referred to in the content.